J.Catal. 237 (2006) 1-16

Preferential CO oxidation in hydrogen (PROX) on ceria supported catalysts
PART I. Oxidation state and surface species on Pt/CeO_2 under reaction conditions

O. Pozdnyakova[1], D. Teschner[1,2]*, A. Wootsch[1], J. Kröhnert[2], B. Steinhauer[2], H. Sauer[2], L. Toth[3], F. C. Jentoft[2], A. Knop-Gericke[2], Z. Paál[1], R. Schlögl[2]

[1]Institute of Isotopes, CRC, HAS, POB 77, Budapest, H-1525, Hungary
[2]Department of Inorganic Chemistry, Fritz-Haber-Institute of the MPG, Faradayweg 4-6, 14195 Berlin, Germany
[3]Research Institute for Technical Physics and Materials Science, HAS, Budapest, POB 49, H-1525, Hungary

* Corresponding author: e-mail teschner@fhi-berlin.mpg.de, phone +49 30 8413 5408, fax +49 30 8413 4676

Abstract

The CO content of hydrogen feed to proton exchange membrane fuel cells (PEMFC) must be kept under 1-100 ppm for their proper operation. This can be achieved by using catalysts able to selectively oxidize CO in the presence of excess hydrogen (PROX). The present study reports on the mechanism of PROX reaction on Pt/CeO_2 catalyst, by using catalytic tests, in-situ DRIFTS, high-pressure XPS, HRTEM and TDS techniques. Bulk metallic, pronounced adsorbate-induced surface Pt and a small amount of oxidized Pt sites were detected by in-situ, high pressure XPS under PROX conditions. The pre-oxidized ceria surface was strongly reduced in pure H_2 but significantly re-oxidized under PROX conditions (i.e. O_2+CO in excess hydrogen) at T=358 K. The remaining small amount of Ce^{3+} decreased with increasing temperature. HRTEM found well-crystallized CeO_2 particles (8-10 nm) in the case of activated (pre-oxidized) sample that transformed in a large extent to an oxygen deficient ceria super-cell structure after PROX reaction. Metallic Pt particles (2-3 nm) and small (0.5-0.6 nm) Pt clusters were found by HRTEM. These findings were in accordance with the variations in relative intensity of the corresponding Pt-CO bands (DRIFTS). Different types of carbonate and formate species were detected (XPS and DRIFTS). Their possible role in the reaction mechanism is discussed. Resolved OH bands could not be found by DRIFT in the PROX reaction mixture indicating significant amount of adsorbed water in a hydrogen-bonded structure. Its presence seems to suppress hydrogen oxidation while CO oxidation still takes place, as the metallic particles are covered by CO (DRIFTS). The direct contribution of surface water in a low-temperature water-gas-shift (LTWGS) type reaction in the PROX mixture is proposed.

Keywords: Hydrogen purification, fuel cell, preferential CO oxidation, PROX, platinum, Pt/CeO_2, ceria, high pressure XPS, in situ DRIFTS, TDS, HRTEM

1. Introduction

Increased attention now turned to development of fuel cell powered systems, because of their expectedly low environmental impact [1]. The Proton Exchange Membrane Fuel Cell (PEMFC) is fueled with clean, CO-free hydrogen, which can be produced by steam reforming (STR), auto-thermal reforming (ATR) or partial oxidation (POX) of natural gas, light oil fractions and alcohols [2,3]. Unfortunately, remarkable amounts, ca. 5-15%, of CO are formed together with H_2, H_2O, CO_2 and CH_4. The concentration of carbon monoxide in the hydrogen feed must be kept below 1-100 ppm for the proper operation of PEMFC [1]. A subsequent water gas shift (WGS) reaction reduces the amount of CO to 0.5-1% [2]. This amount of CO is still high and it can be removed by *pr*eferential *ox*idation (PROX) and/or by methanation of CO using mainly Pt and Pt-Ru bimetallic catalysts [4,5].

Several catalytic formulations have been tentatively tested in the PROX reaction so far. Supported noble metals, such as Au [6-9], Pt [6,9-13], Rh [10], Ru [10,14], and the bimetallic Pt-Sn system [12,15] were found applicable for the reaction. In general, the suitable catalyst must adsorb CO, provide activated oxygen, while hydrogen adsorption must be suppressed. Carbon monoxide is thought to adsorb on the metal phase (Au or Pt), CO adsorption on gold is, however, much weaker than over Pt, manifesting itself in low steady state CO coverage at operational conditions [7,8,9]. On the other hand, oxygen does not adsorb on these metals, either, because the surface is fully covered by CO (on Pt at T<440 K [11,13]) or because of the very low sticking coefficient (on Au [16]). Therefore, oxygen should be activated on different sites: either on the reducible support [6-9,13] or – in the case of modified Pt catalysts – on partially oxidized patches, such as Ru(ox) [14], Sn(ox) [15], Ce(ox) [12] or Fe(ox) [17]. In this way, oxygen should diffuse to interface sites and subsequently react either at the perimeter, or after a spillover process of one of the components on the adjacent metal/oxide site.

The important role of a reducible support manifests itself in the different behavior of Pt/Al_2O_3 and Pt on ceria containing supports in the PROX reaction [13]. Supporting Pt on Al_2O_3 resulted in increasing O_2 conversion and a maximum CO conversion as a function of temperature at around 440 K in the PROX reaction [10,11,13], whereas oxygen conversion on Pt/CeO_2 was very high, even at low temperature and a sharp "light off" activity around 363 K was observed [13]. The maximum in the selectivity as a function of temperature was observed at much lower temperature on Pt/CeO_2 than on Pt/Al_2O_3 and accordingly the maximum CO conversion appeared at a temperature of around 370 K on the former sample [13]. The different behavior of the samples was interpreted by different reaction mechanisms [13]: on Pt/Al_2O_3, a competitive Langmuir-Hinshelwood kinetics can be supposed, since Pt can adsorb all reactants involved. On ceria supported Pt, a non-competitive Langmuir-Hinshelwood mechanism was described: CO activation on Pt particles and their reaction with oxygen activated from the support on the metal/oxide interface at low temperature (T=363-423 K). Both competitive and non-competitive reaction pathways as well as reaction on the ceria support were proposed for higher temperatures [13].

From a more general point of view, cerium oxide is active in transient oxygen storage and, as a catalyst support, it can promote oxidation even under oxygen-poor conditions [18]. Ceria supported platinum [19,20], rhodium [21,22] as well as palladium [23] catalysts were also found remarkably active in the low temperature oxidation of CO, and they were able to oxidize carbon monoxide even in the absence of oxygen, in the so called oxygen storage capacity (OSC) measurement [24,25,26].

A number of publications has been devoted to ceria containing catalysts investigating chemisorptive [27,28], structural [29,30] and catalytic properties [18,31]. Adsorption of CO on ceria supported catalysts leads to accumulation of different carboxylate, carbonate and formate species on the ceria surface as revealed from infrared spectroscopic studies [32-37]. The oxidation state of ceria was also studied after different pretreatments by XPS [38,39,40]. It was found that hydrogen exposure leads to a high concentration of Ce^{+3} at surface and subsurface sites. Moreover, the surface layer of partly reduced ceria easily reoxidizes after exposure to O_2 at room temperature.

A number of direct and indirect experimental evidences has been presented for the reaction mechanism in the PROX reaction on ceria supported Pt [13], nevertheless some controversy and yet unresolved questions exist. For example, what is the surface state of the catalysts during the reaction? Is Pt reduced in the presence of the PROX mixture despite the oxidizing preconditioning? Is the reduction degree of reducible oxides crucial to supply activated oxygen to the reaction? Can the strong temperature dependence of the selectivity on Pt/CeO_x also be explained simply by changes in the CO coverage as was suggested for alloy samples [14,15]? What are the possible surface species formed during the PROX reaction? Are they the same species as in CO oxidation (without hydrogen) or different ones?

In order to gain further insight into the reaction mechanism of the PROX reaction on Pt/CeO_2 catalysts, we examined changes in the oxidation state of ceria and Pt that occur under different reaction environments by high pressure XPS, the surface species formed after adsorption of CO alone, $CO+O_2$ or $CO+H_2+O_2$ (PROX mixture) onto oxidized catalysts by in-situ DRIFTS. In a second communication (Part II) we shall report on Pd/CeO_2 catalysts using the same techniques and as the palladium samples are far less active in the PROX reaction we shall compare the two systems to obtain a better understanding of the reaction mechanism.

2. Experimental

2.1. Catalysts

Two catalysts with nominally 1% and 5% metal loadings were prepared on ceria support (Rhodia Catalysts & Electronics, France, BET=96 $m^2\ g^{-1}$, [41]) by wet impregnation with aqueous solution of $Pt(NH_3)_4(OH)_2$ [13,42]. The impregnated samples were dried at 120°C overnight and calcined for 4 hours at 500°C in flowing air (30 mL/min) and reduced at 673 K for 4 hours in flowing H_2 (30 mL/min). Dispersion was determined by low temperature (223 K) H_2 adsorption after reduction [43,44]. The obtained values were D=62% for 1% Pt/CeO_2 and 18% for 5% Pt/CeO_2.

2.2. Catalysis

Catalytic tests were carried out in an atmospheric continuous flow glass reactor system. Tubing and connections were made from stainless steel. Analytical grade hydrogen, oxygen and CO were used as inlet gases and controlled by Brooks mass-flow controllers previously calibrated. Product analysis was performed by (i) a gas-chromatograph (TCD) equipped with a polar column, Poropak Q, to separate CO_2 and H_2O from the other effluent gases, and (ii) by a hydrogen compensated flue-gas analyzer (MRU DELTA 65-3) for CO and O_2 quantification. Only CO_2 and H_2O were detected as products. Methane did not appear in our experimental conditions. The total gas inlet was 100 NmL/min, containing 1% CO, 0.4-1% O_2 (oxygen excess, λ, from 0.8 to 2) and rest H_2.

Catalysts were activated in situ in flowing air (30 mL/min) at 573 K, before catalytic tests. A charge of 82 mg 1% Pt/CeO_2 and 73 mg 5% Pt/CeO_2 was used in the catalytic reactor and reactivated between different measurement series by the above mentioned treatment [13].

CO and O_2 conversion, as well as the selectivity were calculated as reported previously [13].

The *total conversion* was defined as the oxygen consumption:

$$X_{total} = X_{O_2} = \frac{n_{O_2}^{in} - n_{O_2}^{out}}{n_{O_2}^{in}} \cdot 100 \text{ in \%} \qquad \text{Eq1}$$

The *CO conversion*, considering no side-reactions, can be defined as

$$X_{CO} = \frac{n_{CO}^{in} - n_{CO}^{out}}{n_{CO}^{in}} \cdot 100 = \frac{n_{CO_2}^{out}}{n_{CO}^{in}} \cdot 100 \text{ in \%} \qquad \text{Eq2.}$$

The *selectivity* is defined as the ratio of the oxygen transformed into CO_2 to the total oxygen consumed as:

$$S = \frac{n_{CO_2}^{out}}{2 \cdot (n_{O_2}^{in} - n_{O_2}^{out})} \cdot 100 \text{ in \%} \qquad \text{Eq3}$$

The relation between conversion and selectivity is defined as

$$X_{CO} = \frac{S \cdot X_{O_2}}{100} \cdot \lambda \text{ , in \%} \qquad \text{Eq4,}$$

where lambda (λ) is the oxygen excess factor, by definition:

$$\lambda = \frac{2 \cdot n_{O_2}^{in}}{n_{CO}^{in}} = \frac{2 \cdot p_{O_2}}{p_{CO}} = \frac{2 \cdot [O_2]^{in}}{[CO]^{in}} = \frac{2 \cdot c_{O_2}^{in}}{c_{CO}^{in}} \qquad \text{Eq5.}$$

2.3. Temperature programmed desorption (TDS)

Temperature programmed desorption measurements were performed in a standard UHV apparatus equipped by an atmospheric chamber. The atmospheric part was used to introduce the sample, for pretreatments and adsorbing gases at non-UHV pressures. The 5% Pt/CeO_2 was investigated by TDS. Different gases (gas mixtures) were adsorbed at room temperature on the sample: (i) CO alone (10^{-2} mbar for 30 min), (ii) CO+O_2 (10^{-2} mbar O_2 + $2*10^{-2}$ mbar CO for 20 min), and (iii) H_2+CO+O_2 ($4.7*10^{-1}$ mbar H_2 + $2*10^{-2}$ mbar CO + 10^{-2} mbar O_2 for 20 min). After adsorption the sample was evacuated and transferred to the UHV chamber to follow the desorption pattern. The heating rate was 1 K/s. A Balzers mass spectrometer was used to follow the evolution of desorbing gases.

2.4. In situ diffuse reflectance infrared spectroscopy (DRIFT)

A diffuse reflection attachment "Selector" from Graseby Specac was placed in a Bruker FTIR spectrometer equipped with a D315M MCT detector to collect DRIFT spectra. The spectrometer was purged with purified air. Reactions were conducted in a 2.5 mm high gold cup with 8.5 mm OD and 7.2 mm ID placed in a Graseby Specac "Environmental Chamber" with a ZnSe window. A spectrum of KBr recorded in N_2 served as background. Inlet gases were analytical grade and controlled by mass flow controllers. The total gas inlet was 50 NmL/min, containing 1% CO in N_2 (referred to as *CO alone*), 1% CO, 1% O_2 in N_2 (*CO+O₂*) or 1% CO, 1% O_2 in H_2 (*PROX*).

All measurement series were carried out on ca. 100 mg fresh sample previously pretreated in situ in flowing air (30 mL/min) at 573 K. The catalyst was purged in N_2 while cooling to the desired reaction temperature of 383 or 523 K, respectively. A spectrum of the activated sample before adsorption was collected in N_2 at the reaction temperature and then the reaction mixture – pre-mixed in a bypass – was introduced to the catalyst in one step. Spectra were collected as a function of contact time for 90 minutes in all cases. Only spectra taken under the steady-state conditions will be shown.

Gas composition was analyzed only in the case of PROX reaction by a Pfeiffer Thermostar mass spectrometer. Selectivity and activity values were calculated using the same formula as presented earlier.

2.5. High pressure X-ray Photoelectron Spectroscopy (XPS)

The in-situ XPS experiments were performed at beam line U49/2-PGM2 at BESSY in Berlin. Details about the setup were published [45,46,47]. Briefly, the differentially pumped electrostatic lens system is the key feature of the system, allowing investigating the sample in the mbar pressure region.

The 5% Pt/CeO_2 sample was chosen for these measurements to ensure reliable signal-to-noise ratio in the Pt 4f region. A pressed pellet containing about 100 mg of 5%Pt/CeO_2 catalyst was placed on a temperature-controlled

heater, and was then activated in-situ in oxygen (0.5 mbar, 573 K). Gas flow (~20 NmL/min) into the reaction cell was controlled using calibrated mass flow controllers and leak valves. The PROX mixture contained 0.48 mbar H_2, 0.032 mbar CO and 0.015 mbar O_2. Gas phase analysis was carried out using a quadrupole Balzers mass spectrometer connected through a leak valve to the experimental cell. Selectivity and activity values were calculated using the same formulas as presented earlier.

Ce 3d, O 1s, C 1s, and Pt 4f spectra were recorded with photon energies of hν = 1035, 650 (& 920), 670 and 460 eV respectively. The binding energies were calibrated, if possible, against the Fermi level of the sample or using internal references, such as the Ce 3d V (882.4 eV) and U''' (916.7 eV) hybridization states [48] or the Ce 4f state in the band gap. The energy calibration was necessary because surface charging occurred due to the emission of photoelectrons. In the presence of hydrogen (i.e. in most cases) this was only 1-3 eV, in O_2, however, charging up to 20 eV was observed. Decomposition of the Pt 4f and C 1s regions were performed using Gauss-Lorentz curves. The metallic Pt 4f component at 71 eV was fitted using Gauss-Lorentz profiles with an exponential tail.

2.6. High Resolution Transmission Electron Microscopy (TEM)

HRTEM investigations were performed in a Philips CM200 FEG electron microscope operated at 200 keV. The microscope was equipped with a Gatan imaging filter (GIF 100), Gatan Slow-Scan-Camera and EDX system. The sample was prepared from a piece of the 5% Pt/CeO_2 pellet that was previously activated in O_2 in the in-situ XPS cell as was done for the in-situ XPS experiments. Another sample of 5% Pt/CeO_2 was also investigated after PROX reaction at 358 K (from the XPS cell).

3. Results

3.1. Catalytic reaction

Figure 1 compares the CO oxidation activity on 1% Pt/CeO_2 in the absence and presence of hydrogen. A sharp "light off" activity around 365 K was observed at high oxygen excess without hydrogen, which became less pronounced with decreasing oxygen excess (Figure 1a), in accord with earlier observations [19-21]. In the presence of hydrogen the oxygen conversion (not shown) was very high (around 98-100%), while CO conversion decreased as a function of temperature [13]. The oxygen was consumed for the production of water. Nevertheless, the *natural selectivity* of Pt towards CO oxidation as opposed to H_2 oxidation manifested itself as lower λ values resulted in higher selectivity (Figure 1c).

The catalytic data observed in different experimental setups are compared in Table 1. Unfortunately, the 1% Pt/CeO_2 sample could not be measured by XPS because of the low Pt content. In order to receive well-resolved Pt spectra in the high-pressure XPS apparatus, the 5% Pt/CeO_2 sample was prepared and measured here. DRIFTS results will be mainly shown on the 1% Pt/CeO_2. Both catalysts were tested in the catalytic reactor and 1% Pt showed slightly better performance in the PROX reaction, this difference was, however, negligible (Table 1).

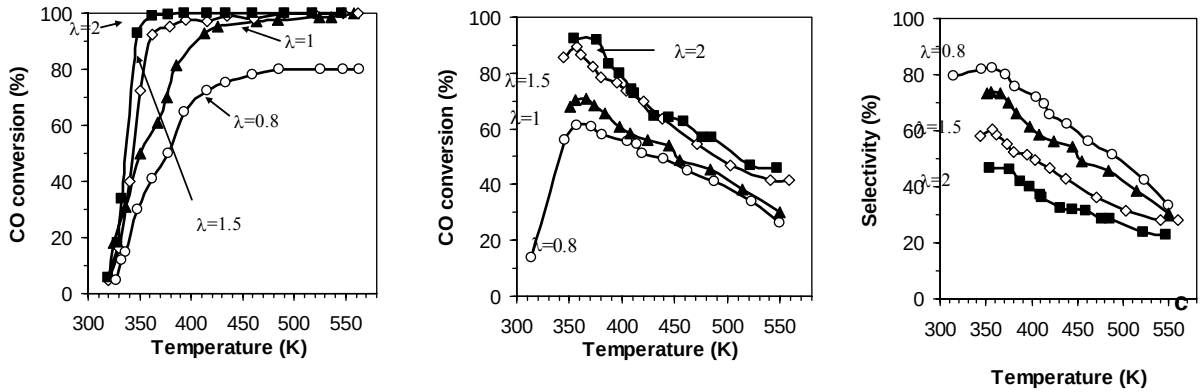

Figure 1: CO oxidation activity in the absence (a) and presence of hydrogen, PROX (b) as well as selectivity towards CO oxidation in the PROX reaction (c) on 1% Pt/CeO_2 catalyst as a function of temperature at different oxygen excess λ. The oxygen conversion was almost total in the PROX reaction under all conditions.

Table 1: PROX reaction in different experimental setups and on different catalysts. Reaction mixtures contained 1% CO, 0.5 or 1% O_2 (O_2 excess λ=1 or 2) in H_2. Total pressure: P=1 atm in catalytic reactor and DRIFTS cell and P=0.5 mbar in high pressure XPS.

Conditions	Catalytic reactor								DRIFTS		XPS	
Catalyst	1% Pt/CeO_2				5% Pt/CeO_2				1%Pt/CeO_2		5%Pt/CeO_2	
O_2 excess (λ)	1	1	2	2	1	1	2	2	2	2	1	1
T (K)	383	523	383	523	383	523	383	523	383	523	358	523
X_{CO}, %	65	38	83	47	59	41	84	42	44	22	9	6
S, %	66	38	42	24	60	41	43	21	30	14	83	18
X_{O2}, %	99	100	99	100	98	100	99	100	73	81	12	38

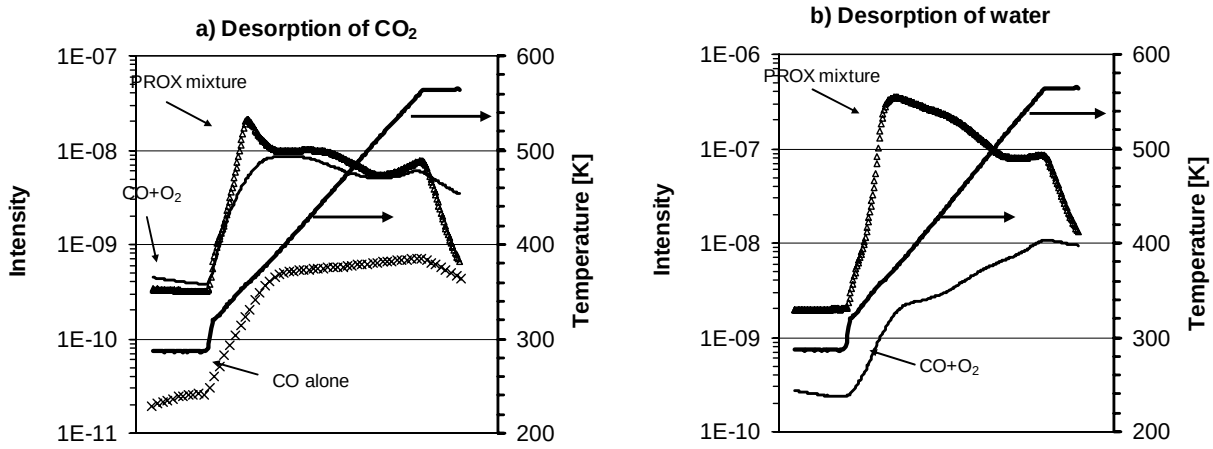

Figure 2: Temperature programmed desorption (TDS) curves of CO_2 (**a**) and water (**b**) from the 5% loading catalyst after adsorbing different gas mixtures at room temperature: CO alone corresponds to 10^{-2} mbar CO for 30 min, CO+O_2 to 10^{-2} mbar O_2 + $2*10^{-2}$ mbar CO for 20 min, and PROX mixture $4.7*10^{-1}$ mbar H_2 + $2*10^{-2}$ mbar CO + 10^{-2} mbar O_2 for 20 min. (Intensities are shown as measured, without calibration.)

Activity patterns measured in different setups showed similar trends, however different actual values (Table 1). In all cases, increasing temperature decreased the selectivity towards CO oxidation and the lower O_2 conversion was, as a rule, accompanied by higher selectivity towards CO oxidation. The differences in the activity pattern can be explained by the different contact times due to the changing dead volume and volume flow-rates in the different experimental setups. In the flow reactor system, sample covers the whole cross-section of the reactor, while in the DRIFT experiments the gas mixture passes over the catalyst powder in a ca. 100 cm^3 cell. In the case of high pressure XPS, the 10 mm diameter pellet was placed in a chamber of ca. 8 liters, and the total pressure was only 0.5 mbar as opposed to the atmospheric pressure used in other setups.

3.2. Temperature programmed desorption (TDS)

Figure 2 shows the desorption curves of CO_2 and water from the 5% loading catalyst after adsorbing different gases or gas mixtures. Formation of CO_2 after adsorption of CO alone is clearly visible. Its amount was, however, an order of magnitude lower than the amount desorbed after oxygen containing mixtures. Interestingly, more CO_2 was produced in the presence of hydrogen, in particular around 358 K. Water desorption was very strongly enhanced after adsorption of PROX mixture especially up to 500 K. Its amount (after calibration) was an order of magnitude higher than expected considering the selectivity values in Table 1.

3.3. In situ DRIFTS

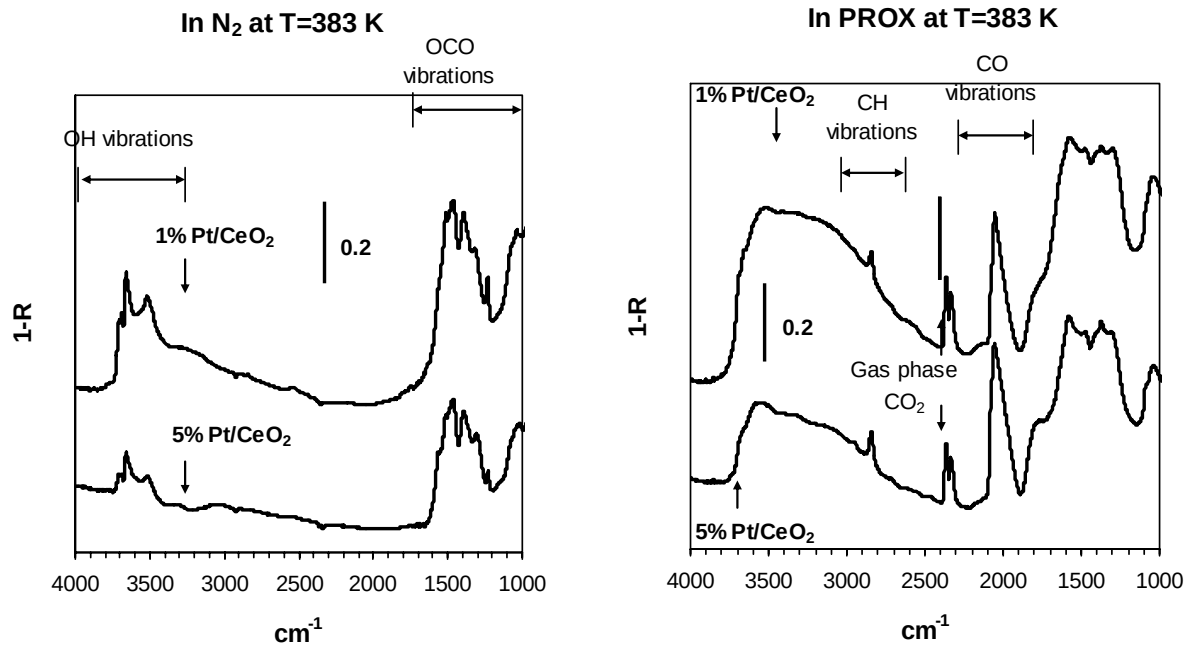

Figure 3: DRIFT spectra of 1% and 5% Pt/CeO_2 at T=383 K **a**) after activation in N_2 and **b**) in the presence of PROX reaction mixture (1%CO, 1%O_2 in H_2).

DRIFT spectra of 1% and 5% Pt/CeO_2 samples recorded after activation in oxygen as well as in different reaction environments (CO alone, CO+O_2 and PROX mixture) exhibited similar features irrespective of the metal loading (Figure 3). Therefore the further discussion will be concentrated to 1% Pt/CeO_2 sample. For clarity, the spectral features observed for four characteristic vibrational regions are presented separately (Figure 4-7), while the characteristic bands corresponding to different surface species are summarized in Tables 2-4.

DRIFT spectra in the region 2200-1700 cm^{-1}

The DRIFT spectra of CO adsorbed on the 1% Pt/CeO_2 under different conditions in the region 2200-1700 cm^{-1} are shown in Figure 4. The bands in this region are summarized in Table 2. Adsorption of CO on Pt/CeO_2 at 383 K in the absence of both oxygen and hydrogen produced one main band at 2063 cm^{-1}, with significant broadening at the low-frequency side, and shoulders at about 2095 and 2083 cm^{-1} (Figure 4a). The strong band at 2063 cm^{-1} and shoulder at about 2083 cm^{-1} could be attributed to linear CO species adsorbed on a step-site and terrace Pt^0 atoms respectively (Table 2) [15,32-35]. The shoulder at ~ 2095 cm^{-1} is due to CO adsorbed on a partly oxidised Pt site in the vicinity of reduced Pt [32-35]. The broad band at ca 1970-1960 cm^{-1} recalls the feature observed at 2000-1960 cm^{-1} on Pt/Al_2O_3, Pt/CeO_2-SiO_2 catalysts and is assigned to CO adsorption at the metal/support interface [49-52]. Kappers et al.[53] attributed this downshift of the ν(CO) band as an indicator of ion-dipole interaction between O atom of the CO species with charged cations from the support. They have shown that adsorbed water can prefentially shield this interaction. A weak ν(CO) band characteristic of bridge-bonded CO species was resolved at 1880 cm^{-1}. An additional weak ν(CO) band observed at ca. 2124 cm^{-1} and a doublet encompassing broad bands at 2172 and 2157 cm^{-1} have previously ascribed to CO linearly adsorbed on reduced and unreduced ceria sites respectively [37,54]. However, in our case these bands overlap with ν(CO) of the gaseous carbon monoxide; and only at ca. 2124 cm^{-1} there is definitely a contribution from adsorbed CO, as the P branch (of gas-phase CO) is weaker than the R branch (above 2143 cm^{-1}).

Increasing temperature led to the (i) decrease in the intensity of the main band and of the shoulder at 2083 cm^{-1} and relative increase in the intensity of the component at ca 1970-1960 cm^{-1}; (ii) shift of the main band to lower wavenumbers (from 2063 to 2051 cm^{-1}); (iii) relative increase in the intensity of the ν(CO) band on Ce^{3+} sites compared to that one on Ce^{4+} sites and (iv) a discernable feature at 2112 cm^{-1}. The broad band at 2112 cm^{-1} is due to CO linearly adsorbed both on Pt atoms interacting with oxygen, i.e. Pt atoms in a more unsaturated coordination state ($Pt^{\delta+}$) [34,35], and on Ce^{3+} sites, respectively.

Table 2: IR bands on ceria supported Pt in the 2200-1800 cm^{-1} region.

	Wavenumbers (cm^{-1})		In N_2		CO alone		CO+O_2		PROX	
Name	Literature values	Our values	110	250	110	250	110	250	110	250
CO adsorbed on Ce^{4+}	2177, 2156 [37], 2170-2127 [54]	2172-2154	-	-	+	+	+	+	low	+
CO adsorbed on Ce^{3+}	2120-2127 [54]	2124	-	-	Always present,					
CO adsorbed on Pt(ox)	2122-2131 [35]	2121-2115	-	-	their distinction is difficult					
CO adsorbed on metallic Pt with Pt(Ox) neighbor	2091-2096 [34,35]	2095	-	-	+	low	+	low	low	low
CO linearly adsorbed on terraces	2080 – 2085 [14,15,34,35]	2083-2075	-	-	+	+	+	+	+	+
CO linearly adsorbed on step sides	2072-2065 [14,15,34,35]	2068-2041	-	-	+	+	+	+	+	+
CO on metal/support interface side	1960-1970 [33,49-52]	1960-1970	-	-	Always present, more at high T					
Bridged CO on Pt	1850 [14,33]	1877-1882	-	-	Only small amount at low T					

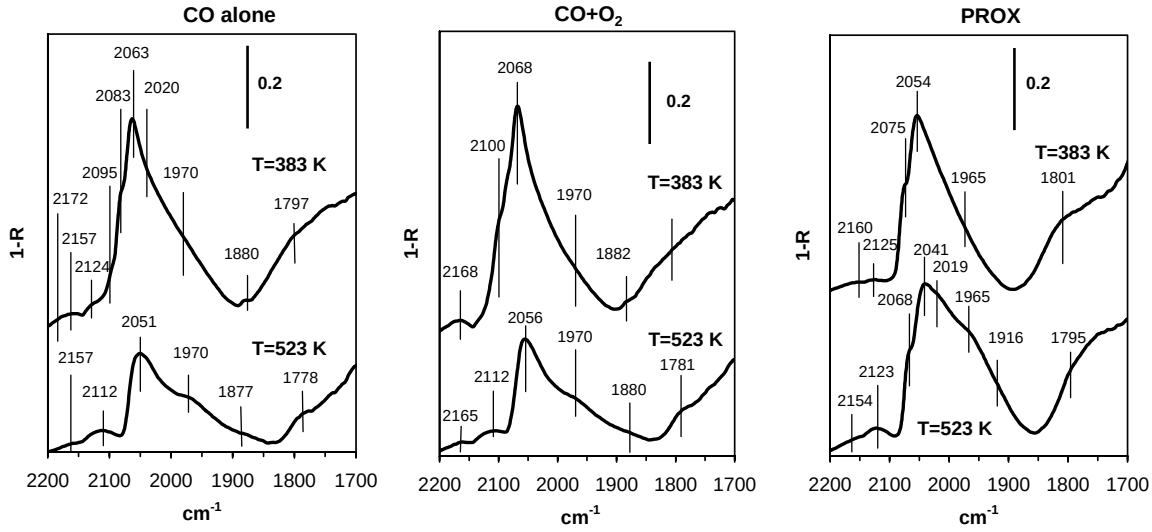

Figure 4: DRIFT spectra in the 2200-1700 cm^{-1} region - CO vibrations - of 1% Pt/CeO_2 in the presence of a) 1% CO alone in N_2 b) in 1% CO and 1% O_2 in N_2 and c) in 1% CO and 1% O_2 in H_2 - PROX at 383 and 523 K, respectively.

In the presence of oxygen in the gas mixture (Figure 4b) only moderate changes occurred as compared to the CO alone case (Figure 4a): most of the ν(CO) bands were slightly blue-shifted (~5 cm^{-1}), the intensity of the shoulder at 2095 cm^{-1} relatively increased and that one at 2083 cm^{-1} decreased. These changes can be explained by slight oxidation (probably hindered reduction) of the Pt particles.

Under PROX conditions (Figure 4c), a general shift to lower wavenumbers was observed with the main band shifted from 2063 to 2054 cm^{-1} and the shoulder being positioned at 2075 cm^{-1}. Increasing temperature in the presence of hydrogen resulted in further shift of these ν(CO) bands to 2041 and 2068 cm^{-1}, respectively, and relative increase in the intensity of the broad ν(CO) band at 1965 cm^{-1}, as compared to T=383 K.

DRIFTS spectra in the region 1800-1000 cm^{-1}

The DRIFTS spectra of the 1% Pt/CeO_2 sample under different conditions in the region 1800-1000 cm^{-1} are shown in Figure 5. In this region different carbonate, carboxylate and formate species gave several bands; their assignments are summarized in Table 3 and 4. The identification of carboxylic acids, bicarbonates and formate species were also based on their other characteristic O-H (Figure 6) or C-H bands (Figure 7), respectively.

Unidentate carbonate (strong bands at 1464 and 1358 $cm^{-1}$and weak band at 1080 cm^{-1}), bidentate carbonate (features at ca. 1565, 1300 and 1013 cm^{-1}) and traces of bicarbonate (medium bands at 1393, 1232, weak band at ca 1050 and shoulder at ca 1611 cm^{-1}) and carboxylate

Table 3: IR bands on ceria supported Pt for carbonate and carboxylate species. Bands in italic are OH vibrations

		Wavenumbers (cm^{-1})		In N_2		CO alone		$CO+O_2$		PROX	
Name	formula	Literature values	Our values	110	250	110	250	110	250	110	250
Carbonate unidentate	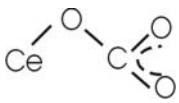	1545, 1348, 1062 [36]	1464, 1358, 1085	+	+	+	+	+	+	+	+
Carbonate bidentate	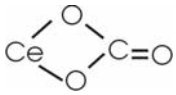	1562, 1286, 1028 [36]	1565, 1298, 1014-1009	+	+	+	+	+	+	+	+
Carbonate polyden-tate	Polymer	1462, 1353, 1066 [36]	1463, 1353, 1050-1040	+	+	+	+	+	+	+	+
Bridged carbonate	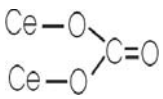	1728, 1396, 1219, 1132 [36]	1740, 1393, 1232, 1145	+	-	+	-	+	-	-	-
Bicarbon-ate	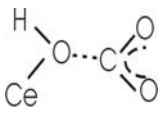	3617, 1613, 1391, 1218, 1045 [36]	3619, 1611, 1393, 1217, 1043	-	-	+	-	+	-	-	-
Carboxy-late	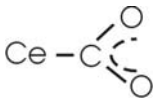	1560, 1510, 1310 [36]	1514, 1316	+	+?	?	+	?	+	-	-
Carboxylic acid	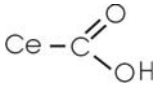	1670-1695,1338-1310 [35,36]	3590, 1700-1600, 1335	-	-	+	+	+	+	+	+

Table 4: IR bands on ceria supported Pt for formate and -OH species. Bands in italic are OH or CH vibrations

		Wavenumbers (cm^{-1})		In N_2		CO alone		$CO+O_2$		PROX	
Name	formula	Literature values	Our values	110	250	110	250	110	250	110	250
Bidentate formate	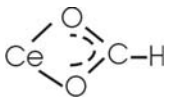	2945, 2852, 1558, 1369, 1329 [37] 2845, 1547, 1358 [55]	2936, 2848, 1545, 1372, 1360	-	-	+	+	-	+	+	+
Bridged formate	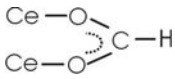	2933, 2852, 1575, 1358 [55], 2945, 1587, 1329 [37]	2950, 2844, 1582, 1372, 1330	-	-	+	+	-	+	+	+
Type I OH	Ce-OH	3710 [33,59]	3708-3700	+	+	+	+	+	+	?	+
Type II-A OH	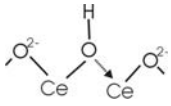	3650 [59] 3680-3660 [33,58]	3658-3667	+	+	+	+	+	+	?	+
Type II-B OH	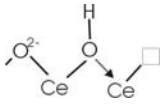	3651 [33,58]	3619-3625	+?	+	+?	+	-	+	?	+
Type III OH	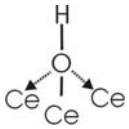	3500 [59], 3600 [33,58]	3517	+	+	+	+	+	+	+	+

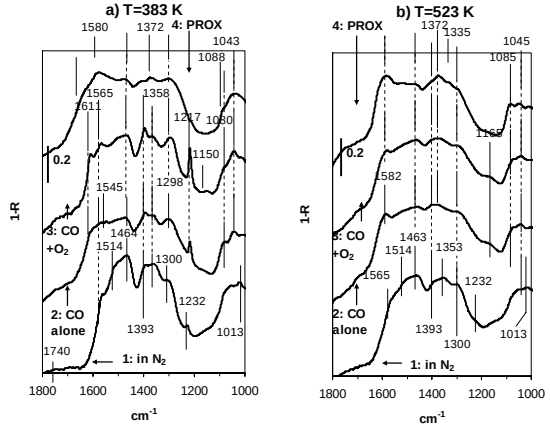

Figure 5: DRIFT spectra in the 1800-1000 cm^{-1} region - OCO vibrations - of 1% Pt/CeO_2 at a) T=383 K and b) T=523 K after activation, in the presence of 1% CO alone in N_2, in 1% CO and 1% O_2 in N_2, and in 1% CO and 1% O_2 in H_2 - PROX, respectively.

(feature at ca. 1514 and very weak band at 1316 cm^{-1}) species were present on the surface of the O_2 pre-treated sample at T=383 K in N_2 (Figure 5a). Increasing temperature resulted in a decrease of the bicarbonate and slight increase of the bidentate carbonate species on the surface of the activated sample (Figure 5b).

Exposure to 10 mbar of CO alone or in the presence of oxygen yielded bands that were grouped as follows: (i) strong bands at 1393, 1217 and weak ones at 1611 and 1043 cm^{-1}, (ii) strong broad band at 1298, weak ones at 1565 and ~1010 cm^{-1}, and (iii) medium band at 1545 and weak ones at 1372 and 1360 cm^{-1}. The first group of bands was assigned to bicarbonate species, which correlates well with the appearance of strong ν(OH) band at 3619 cm^{-1} and concomitant decrease of another OH band (see next section, Figure 6) observed upon exposure of sample to CO or CO+O_2 gas mixtures. The second group of bands belongs to bidentate carbonate species. The relative intensities of the bands of different carbonate species were not affected by the presence of oxygen in the gas mixture, except for bands of bicarbonate, which were enhanced in CO+O_2 atmosphere. The third group of bands appearing only in the presence of CO alone, complemented by the appearance of ν(CH) bands, to be discussed later (Figure 7), belongs to bidentate formates formed on partially reduced ceria through reaction between CO and surface hydroxyl groups [37].

Under PROX conditions bicarbonate species observed in H_2-free gas mixtures did not form (Figure 5). The ν(OCO) bands of bidentate formate species became poorly resolved with overall decrease in intensities. At the same time, a strong broad feature develops at ca 1582 cm^{-1}, which might be attributed to the ν_{as}(OCO) band of bridged formate species [55]. The significant broadening above 1611 cm^{-1} corresponds to surface water (see later). The ν(CO_3) bands of bi- and unidentate carbonate species of similar intensities were present in the spectra in H_2-rich atmosphere.

At T=523 K, the presence of CO alone and CO+O_2 gas mixtures gave a strong band at 1582 and weak ones at 1372, 1540 and 1360 cm^{-1} (Figure 5b), which were accompanied by the simultaneous appearance of a strong ν(CH) band at 2850 cm^{-1} (Figure 7). These features indicate that bridged formate and probably traces of bidentate formate species are present on the surface. Under PROX conditions at T=523 K bands belonging to bridged formate species (1582, 1372 and 1330 cm^{-1}) significantly increased as compared to at T=383 K in the presence or at T=523 K in the absence of H_2.

Ill-defined bands due to uni- and/or poly- [56] and bidentate carbonate species were also observed at T=523 K. Under PROX conditions, the poorly resolved bands at 1335, 1690, and 1510-1506 cm^{-1} (Figure 5) reflect the presence of protonated carboxylate species, carboxylic acid (-COOH) on the surface as also indicated by the corresponding ν(OH) 3590 cm^{-1} (Figure 6) .

DRIFT spectra in the region 3800-3100 cm^{-1}

Four OH groups were reproduced after oxidative activation on the 1% Pt/CeO_2 sample at T=383 K as shown in Figure 6a. They are denoted as type I, II or III according to the number of cerium cations constituting the adsorption site [57]. The sharp peak at 3704 cm^{-1} was assigned to mono-coordinated OH (Type I), the band at 3651 cm^{-1} with the shoulder at ca. 3625 cm^{-1} has been assigned to two types of bridging OH (Type II-A and II-B, respectively), while a broad band centred at 3517 cm^{-1} was assigned to triply bridging OH (III) species (Table 4) [58,59]. At T=523 K, a slight down-shift of all ν(OH) bands and decrease in the number of mono-coordinated (OH-I) and doubly bridging (OH-II) hydroxyl groups on the ceria surface was observed (Figure 6b).

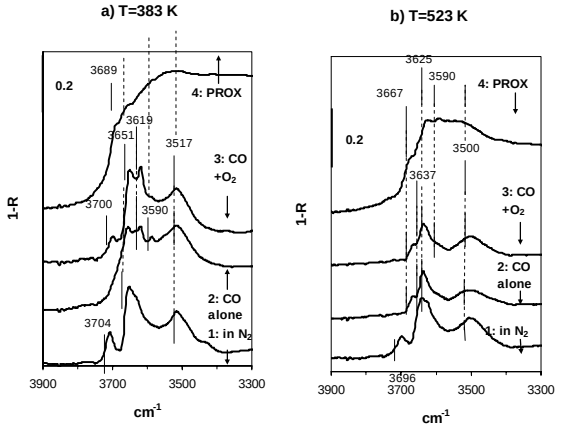

Figure 6: DRIFT spectra in the 3900-3300 cm^{-1} region - OH vibrations - of 1% Pt/CeO_2 at a) T=383 K and b) T=523 K after activation, in the presence of 1% CO alone in N_2, in 1% CO and 1% O_2 in N_2, and in 1% CO and 1% O_2 in H_2 - PROX, respectively.

The presence of CO alone or O_2+CO at T=383 K (Figure 6a) resulted in (i) appearance of ν(OH) bands at 3619 cm^{-1} and at 3590 cm^{-1}; and (ii) decrease in the intensity of the ν(OH-I) band at 3704 cm^{-1}. The development of a strong band at 3619 cm^{-1} and decaying of band at 3704 cm^{-1} were attributed to the formation of HCO_3^- species through reaction of CO with terminal (OH-I) hydroxyl groups (accordingly bicarbonate vibrations on Figure 5 were found and discussed earlier). The other developed ν(OH) band at 3590 cm^{-1} might reflect the presence of carboxylic acid (-COOH) groups on the surface of the ceria support, because it correlates with the weak broad features observed under the same conditions at ca. 1690, 1510-1506 and 1330 cm^{-1} (Figure 5). Decreasing ν(OH) bands can be correlated with the development of formate species as described later.

The presence of oxygen had little effect on the position and relative intensities of the ν(OH) bands, only the intensity of the band at 3704 cm^{-1} was enhanced in the presence of oxygen as compared to in CO alone gas mixture (Figure 6a).

After CO adsorption at T=523 K no distinct ν(OH) band of bicarbonate species was resolved, while ν(OH) stretching of all surface hydroxyl groups were down-shifted (~10 cm^{-1}) as compared to at T=383 K.

Under PROX conditions at T=383 K isolated bands become convoluted into intense and broad adsorption features, among which those centred at ca. 3689, 3658 (OH-IIA) and 3590 (carboxylic acid) could be somewhat resolved. Decrease in resolution and general broadening of the stretching ν(OH) and a strong increase in absorption towards lower wavenumbers indicate considerable H-bonding. A band at ca. 1640 cm^{-1} and the observation of H_2O as a product are further evidence for the presence of significant amounts of water on the surface. H-bonding with the Ce-OH groups suggests that the water is predominantly adsorbed on the support. Increasing temperature under PROX conditions decreased the intensity of features caused by adsorbed water and gave increase in the intensity of the bands at 3625 cm^{-1} (OH-IIB) and 3590 cm^{-1}.

DRIFT spectra in the region 3000-2600 cm^{-1}

The main bands in this vibration region can be assigned to bridged and bidentate formate species as follows (Figure 7): 2848 cm^{-1} as ν(CH), 2936-2950 cm^{-1} as combination of ν_{as}(OCO) and the C-H in-plane vibration, 2719 cm^{-1} as overtone 2δ(C-H), which around δ(C-H)=1360 cm^{-1} is, indeed, hardly visible because of the strong carbonate vibrations (Figure 5). The C-H vibrations of the two different formate species, bidentate and bridged, are quite similar, however the difference in ν_{as}(OCO) - ~1545 cm^{-1} for bidentate and ~1582 cm^{-1} for bridged (Table 4) [37,55] - makes their distinction possible. Consequently, the combination mode of ν_{as}(OCO) and the C-H in-plane vibration should also be higher for the bridged species than for the bidentate one [60].

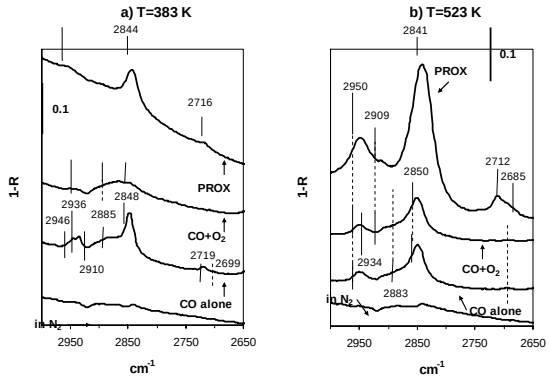

Figure 7: DRIFT spectra in the 3000-2650 cm^{-1} region - CH vibrations - of 1% Pt/CeO_2 at a) T=383 K and b) T=523 K after activation, in the presence of 1% CO alone in N_2, in 1% CO and 1% O_2 in N_2, and in 1% CO and 1% O_2 in H_2 - PROX, respectively.

After oxidative treatment of the Pt/CeO_2 sample no bands were observed in the region 3000-2600 cm^{-1}, while in CO stream, strong bands at 2936 and 2848 cm^{-1} and weak features at ca. 2910, 2719 and ca 2699 cm^{-1} appeared (Figure 7a). The main bands were assigned to surface formate species [37,61,62], mainly to bidentate formate (see above). Surface formate species on ceria were proposed to be formed through reaction of CO with terminal (OH-I) [55] and/or bridging (OH-II) [37,63] hydroxyl groups, accordingly these OH band decreased as discussed in the preceding section. The spectra under conditions of CO+O_2 exhibit no distinct bands in the 3000-2600 cm^{-1} region. In the PROX gas mixture, at T=383 K because of the strong "hydrogen bonded OH-water structure" the background is increasing as a function of wavenumbers, and thus bands are poorly resolved. Nevertheless, a ν(CH) band at 2844 cm^{-1} was observed accompanied by weak broad features at ca 2716 and 2952 cm^{-1}. They might reflect the presence of both bidentate and bridged formate species on the surface (the latter probably being in excess, see corresponding ν_{as}(OCO) – Figure 6) or/and imply that the broad band at 2844 cm^{-1} probably involves some contribution from ν(CH) vibrations, which are not associated with the formate species (hydrocarbonaceous residue).

At T=523 K, under conditions of CO alone and CO+O_2 the position of the main ν(CH) band at 2848 cm^{-1} was hardly affected. However, the ratio of bridged and bidentate formate species seemed to change, more bridged and less bidentate formate could be estimated than at low temperature; because of the relative increase in the intensity of the band at 2950 cm^{-1} and significant decrease in the intensity of the band at 2936 cm^{-1}, in accordance with the position of the corresponding ν_{as}(OCO) bands (see earlier). The presence of hydrogen in the gas mixture at elevated temperature resulted in (i) significant increase in the intensity of bands belonging to bridged formate species and (ii) appearance of several weak bands, that might be assigned to ν(CH) band of formyl species or could originate from different other CH-containing species.

3.4. High pressure XPS

The 5% Pt/CeO_2 sample was investigated in different gaseous ambient using our novel high-pressure XPS setup [46,47]. The sample was first activated in 0.5 mbar O_2 at 573 K. Thereafter it was cooled down in O_2. At ~340 K oxygen was evacuated and replaced by hydrogen (0.48 mbar). As the ambient temperature was reached, first CO (0.032 mbar) and then O_2 (0.015 mbar) was added to the hydrogen. The surface state of the sample was investigated in these different environments. The catalytic activity observed during high-pressure XPS measurements was presented in Table 1.

Figure 8 depicts a part of the Ce3d region in oxygen (573 K), in hydrogen (300 K) and in the PROX mixture at 358 K. As expected, the surface of ceria was more or less completely oxidized in oxygen whereas hydrogen induced the formation of Ce^{+3} species. The peaks V^0 and V' at ~ 880.7 and ~ 885.5 eV, respectively are characteristic for Ce^{+3} species, while V and V'' (~882.4 and ~888.7 eV) correspond to oxidized ceria. (The same notation is used as established by Burroughs et al. [48] and popularly applied in other papers[38,39] as well.) The use of 1035 eV synchrotron radiation ensures - due to the low KE electrons (~140 eV in this part of the spectrum) - that mainly the topmost few (2-3) Ce layers were probed. The reduction degree of ceria in hydrogen was estimated to be roughly about 50%. Assuming that the reduction at low temperature affects just the top layer, this layer should be fully reduced to Ce^{+3}. In the PROX mixture, however, the surface is clearly re-oxidized. Please note that the gas mixture contains just 3% oxygen, while the other 97% has a reducing character. This re-oxidation was slightly more pronounced at 523 K, therefore oxygen has a very strong sticking probability on ceria surfaces even at higher T. The ratio of V-to-V'' hybridization states changed in the PROX reaction mixture, although the surface was more or less similarly oxidized as in pure O_2.

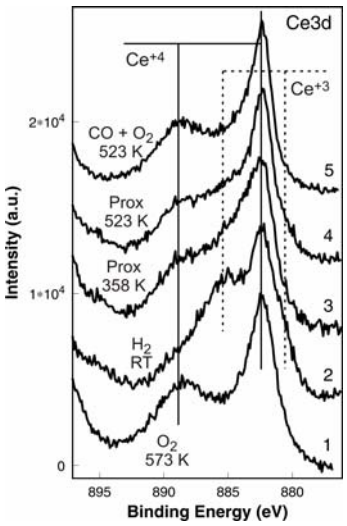

Figure 8: Part of the Ce 3d region of the 5% Pt/CeO_2 at different conditions: 1, in 0.5 mbar O_2 at 573 K; 2, in 0.48 mbar H_2 at RT; 3, in ~ 0.5 mbar PROX mixture at 358 K; 4, in ~ 0.5 mbar PROX mixture at 523 K; 5, in a mixture of 0.032 mbar CO and 0.015 mbar O_2 (as hydrogen was switched off after 4,) The measurements were carried out in sequence as indicated by the numbers.

Figure 9a shows the platinum 4f core level in hydrogen and in the reaction mixture at two different temperatures. In oxygen, charging of about 17 eV made the platinum peak (not included in the figure) too broad to evaluate its form. However, introduction of hydrogen at close to room temperature may induce hardly any changes in the valence state of platinum, thus we consider this spectrum as representative for the oxygen activated sample. The spectrum indicates two distinct components; one is in the zero-valent state, while the other shows a binding energy shift of +1.6 eV. The identification of this second component according to the literature is controversial. In several studies a Pt^{2+} state (e. g. PtO) was found in +1-1.8 eV relative to metallic Pt [64,65]. However numerous others [66,67] indicate PtO in a +2.4-3 eV distance and PtO_2 is observed in +3.6-4.5 eV distance [66,68]. Different surface-core-level-shift (SCLS) values were observed for adsorbed O_2 on Pt single crystals [67,69]. At this point, without arguing in favor of any of these possibilities, we will call this component "Pt-oxidized1". At 358 K under PROX conditions the spectrum changed appreciably, as this component was not resolved anymore and a shoulder at 72.0 eV appeared. The 7/2-to-5/2 splitting is still not well separated (intensity at ~ 73.5 eV), therefore the Pt-oxidized1 component should not completely disappear. Moreover a tail at around 77.2 eV is now well detectable, which indicates a not resolvable 7/2 component at ~ 73.9 eV. This will be termed as Pt-oxidized2. According to the literature [69], SCLS of adsorbed CO give a BE shift of ~ +1.0 and +0.4 eV, identified as on-top and bridged bonded CO, respectively. Therefore we may identify the 72.0 component as Pt with linearly bonded CO. On the other hand, the fraction of this Pt species is too high to be explainable solely by surface Pt, as the spectra were taken with 460 eV photons, i.e. not surface sensitive enough to account for such intense component. One possible explanation could be that some special CO induced compound-like platinum atoms give rise this Pt 4f peak, or the particles are extremely small and additional surface reconstruction occurs. Bridged CO cannot be resolved from our spectrum. Upon heating the sample further to 523 K, the new peaks disappeared and the spectrum resembled well that measured after activation. The Pt-oxidized1 state slightly decreased in the reaction mixture.

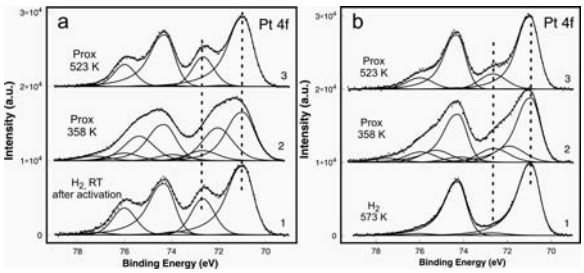

Figure 9: Pt 4f region of 5% Pt/CeO_2 at different conditions: 1, in 0.48 mbar H_2 at RT (after O_2 activation at 573 K); 2, in ~ 0.5 mbar PROX mixture at 358 K; 3, in ~ 0.5 mbar PROX mixture at 523 K; Figure 9**b** 1, in 0.48 mbar H_2 at 573 K; 2, in ~ 0.5 mbar PROX mixture at 358 K; 3, in ~ 0.5 mbar PROX mixture at 523 K. The measurements were carried out in sequence as indicated by the numbers.

In the second experiment, the sample after activation was reduced in hydrogen at 573 K, and was tested in the PROX reaction. The catalytic behavior of sample was comparable to the non-reduced one, showing similar activity at low T and selectivity decay at 523 K. The corresponding spectra are shown in Figure 9b. Platinum was totally reduced during the 573 K hydrogen treatment and could be fitted with the typical asymmetric function. In the PROX reaction mixture at low T, all the above-mentioned components appeared, only their relative intensities were smaller. This indicates that the Pt-oxidized1 species can be formed in the reaction mixture already at 358 K (or lower). Considering the high excess of reducing gases (H_2 and CO), the identification of this component as "bulk" PtO is not likely. It is more possible that under less severe, reducing conditions, the interface atoms are polarized by the negatively charged anions of the supporting ceria. If so, the Pt particles should be very small (few nm, or even smaller).

Carbon 1s spectra of the activated sample in the reaction mixture at low and high temperature are shown in Figure 10. Due to the variation in the form of the spectra we used several components (actually, 7 is shown) to adequately fit the measured curves. However, the unambiguous assignment is hardly possible, since many different species can have very similar binding energy [70]. As a first approximation we consider the lowest BE peak (284.2 eV) as graphene or graphite, the peaks around 286 eV as adsorbed CO in bridged (285.6 eV) and in linear (286.3 eV) coordination to Pt, the other high-BE peaks (except that of 290.6 eV, which is gas phase CO) as different oxidized carbon on Pt, but mainly on the ceria surface. As only a negligible amount of bridged CO (bonded between two Pt atoms) was detected by DRIFTS, the species at 285.6 may rather belong to CO bonded to the Pt/ceria interface (CO band at ~1960 cm^{-1}). This interface CO can, however, be regarded as bridged adsorbed CO as well, considering that C is coordinating to Pt and O is interacting with a coordinatevely unsaturated (cus) Ce^{n+} site.

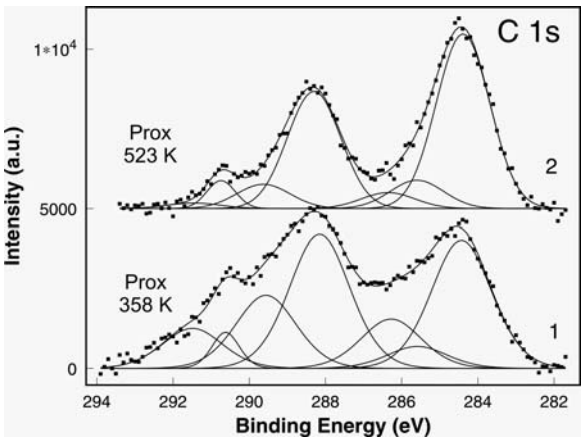

Figure 10: C 1s region of 5% Pt/CeO_2 at different conditions: 1, in ~ 0.5 mbar PROX mixture at 358 K; 2, in ~ 0.5 mbar PROX mixture at 523 K.

3.5. High Resolution Transmission Electron Microscopy (TEM)

High resolution TEM measurements were performed on the activated 5% Pt/CeO_2 to characterize the microstructure of the sample and to try to identify oxidized Pt (see above). The ceria particles (8-10 nm) were strongly stacked together despite the careful sample preparation, allowing no phase identification in most of the area of the specimen. Furthermore, depicting platinum particles is widely hindered by the strong contrast of the ceria lattice. Therefore very few Pt particles could be found. A selected image is shown in Figure 11a, on which accidentally two Pt particles can be seen. The particle with a size of about 2x3 nm is [110] oriented, which can be deduced from its power spectrum (inset). (The power spectrum is the square of the modulus of the Fourier Transform of the two-dimensional image (or a chosen part of the image) and represents the (computer generated) diffraction pattern of the image.) The contrast of the particle was slightly enhanced by filtering

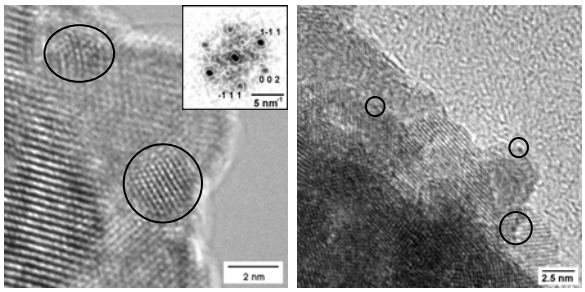

Figure 11a: High-resolution TEM image of 5% Pt/CeO_2 after activation in oxygen at 573 K. The inset shows the power spectrum of the platinum particle situated in the middle of the TEM image. **Figure 11b**. Other section of the sample showing very small dark spots (indicated by circles) that might correspond to Pt clusters in the size of 5-6 Å.

the corresponding spots (inverse lattice fringes) of the power spectrum, back-transforming and adding it to the original image. Figure 11b shows another part of the sample in which unidentified dark spots can be seen on the surface of ceria. These spots did not behave like the dark and light spots in the carbon foil (*flickering*), therefore they do not belong to the foil, but might be very small (5-6 Å) Pt clusters. If so, they should be partially oxidized through the relatively strong interaction with ceria. Oxidized "bulk" platinum however could not be found in any form on the images. Therefore we identify the 72.6 eV Pt 4f component as small Pt clusters (or interface Pt atoms) strongly interacting with ceria. Most of the ceria particles were in the form of CeO_2 (fluorite structure) with [110], [111] and [001] orientation. In some cases a small lattice expansion and a stronger angular distortion could be calculated mainly because some defective structure. Additionally, EDX measurements were carried out to roughly characterize the bulk Pt content of the sample. Using an area of 300 nm in diameter, the calculated Pt content was ~4 weight %. Using several small (13 nm) regions, calculation gives a minimum value of 4 % and max. value of 5.3 w%, thus platinum should be quite homogeneously distributed in the sample.

HRTEM after PROX reaction found a markedly higher number of reduced ceria particles with a more pronounced reduction degree. Careful analysis of the ceria particles revealed an oxygen deficient structure ($CeO_{1.695}$), in which the vacancies ordered and formed a super-cell. Its lattice constant is more than twice that of CeO_2. For further details, see Part II.

4. Discussion

Interaction of *CO alone* with the pre-oxidized catalyst can be seen in DRIFT spectra mainly as CO bonded to the metallic particles (Figure 4). This adsorbed CO can then react with spilt over oxygen to form gas phase CO_2 (observed in that times in the gas phase spectra during DRIFTS experiments but not shown) [24,25,26,44]. The TDS measurement of adsorbed CO (Figure 2) confirms this model. CO adsorbed on ceria sites and/or spilt over from the metal to the support is present only in a low proportion (Figure 4), while a pronounced increase in the carboxyl region at 1800-1000 cm^{-1} was observed (Figure 5). Thus CO on support sites must have oxidized rapidly to form different types of carbonate species [44], the pronounced CO_2 desorption upon CO adsorption in the TDS spectra (Figure 2) also supports this idea. At the same time, the interaction of CO species with the support OH groups (3704 cm^{-1}) results in the formation of formate and bicarbonate species clearly seen in Figures 5-7.

In the case of CO oxidation with oxygen mainly the same changes were observed in the DRIFT spectra in experiments with CO alone. The only difference was that the ν(CO) bands between 2060-2100 cm^{-1} were slightly blue-shifted and that bands in the C-H region were less pronounced when oxygen was present. They even disappeared at T=383 K. Thus, the presence of oxygen

(i) hardly affected CO adsorption and

(ii) suppressed the formation of C-H bands.

The first observation indicates that the reaction mechanism (surface species) must have been the same in the experiments with CO alone and CO+O_2. The role of oxygen was limited to re-oxidation of support sites, because the Pt particles were almost totally covered with CO, as postulated earlier [18,24,25,26]. It correlates well with the observed strong affinity of partly reduced ceria surface towards gas phase oxygen: it can be re-oxidized even at low temperature (T=358 K) in the presence of the PROX mixture - 3% O_2 - (see Figure 8). Accordingly, the participation of oxygen from the ceria support in CO oxidation was proved earlier both (i) from observation of zero order oxygen pressure dependence [23] and (ii) by oxygen-exchange measurements between $C^{16}O$ and ^{18}O-pre-dosed catalysts [21].

Disproportionation of carbon monoxide $2CO \rightarrow C+CO_2$ was also reported to be a reaction pathway for the OSC measurement on Pt/CeO_2 at high temperature [44]. The spillover and interaction of this carbon species with OH groups can also result in the formation of bands in the region of CH vibrations. Nevertheless, the reaction mechanism of CO disproportionation is not clarified. In fact, this process can take place via dissociation of CO and then reaction of the left over oxygen with another adsorbed CO molecule.

The suppression of C-H bond formation is due to the fact that excess oxygen present in the gas phase may re-oxidize these species to carbonates or to CO_2. However, at high temperature concomitantly with the evolution of these bands, the formation of gas phase CO_2 is suppressed (Figure 12). The additional increase in the C-H region is not attributed to formates, but rather to methylidyne or partly hydrogenated graphitic species (Figure 10) formed after CO dissociation.

In the presence of the PROX reaction mixture, a completely different picture is observed in the OH region of DRIFT spectra (Figure 6). Not well-resolved overlapping curves were observed at T=383 K, indication of strong hydrogen bonded system on the surface. Accordingly, XPS of the O1s region indicated also a pronounced amount of adsorbed water on the ceria surface at low temperature (see Part II, in comparison with Pd/CeO_2). At the same time, ceria is only slightly reduced at low T (Figure 8).

Before drawing the reaction mechanism for the PROX reaction, it must be emphasized that Pt itself is active both in hydrogen and CO oxidation, and an obvious reaction route is that products of these reactions, CO_2 and H_2O desorb from Pt and the selectivity is determined only by the competitive adsorption of CO, H_2 and O_2, as was clearly shown for the Pt/Al_2O_3 system [11,13]. In this case hydrogen adsorption on Pt, hence the possibility towards non-selective oxidation, is strongly suppressed by the high (however not total) CO coverage, even in excess H_2. Nevertheless, Pt/CeO_2 shows different behavior from Pt/Al_2O_3

in the PROX reaction [13], as it was already emphasized in the Introduction.

Our results show that accumulation of both CO_2 (in the form of carbonates and formates) and H_2O (in "hydrogen bonded OH-water structure") is possible on the ceria support, especially at lower temperatures. These structures can be formed either by spillover of reaction products (CO_2 and H_2O) or – which is more probable – by spillover of hydrogen or CO to the support. The possibility of direct adsorption (for example of H_2 [71]) on the support cannot be neglected either. Among all, the probability of hydrogen spillover is, in fact, highest. This hydrogen on the support reacts rapidly with oxidized ceria to form OH groups on the surface, while ceria is reduced to Ce^{3+} and adsorbed water accumulates on the ceria surface. This water then reacts with carbonate and carboxylate groups present and hydroxylation of the surface takes place (see the relatively high amount of carboxylic acid in the PROX reaction, as observed by DRIFTS). The reduced Ce^{3+} centers on the surface seem to be re-oxidized. HRTEM indicates, however, that these reduced defect sites formally move into the bulk of ceria forming an oxygen deficient super-cell during the reaction. The presence of adsorbed water seems to suppress hydrogen oxidation while CO oxidation still takes place, as the metallic particles are covered by CO, and most probably because oxygen spillover to the metallic site is not hindered by this hydrogen bonded structure. The promoting effect of surface water on CO oxidation over Pt catalysts was postulated recently upon microkinetic modeling [72]. The possibility of a direct contribution of water in a low-temperature water-gas-shift type (LTWGS) reaction was also proposed [72]. This way, surface water (and/or OH groups) would react at the perimeter of Pt particles with linearly bonded CO molecules [72], or with surface formate [63,73], or carboxyl species [72], which are thought to be intermediates in LTWGS reaction producing CO_2 and H_2. Each of these possibilities would result in relatively high selectivity towards CO oxidation in PROX at low temperature.

Increasing the temperature in the PROX reaction leads to

(i.) decrease of selectivity towards CO oxidation (Figure 1 and Figure 12),
(ii.) further oxidation of the ceria surface (Figure 8),
(iii.) decrease of the linearly adsorbed CO species seen both in XPS (Figure 10) and DRIFT (Figure 4),
(iv.) increase of the band around 1965 cm^{-1} (Figure 4),
(v.) increasing intensity of C-H vibrations in the DRIFT spectra (Figure 7),
(vi.) increasing amount of graphite-like species in the C1s XPS spectra (Figure 10),
(vii.) decrease of surface OH-water H-bonded structure (Figure 6).

The interaction of CO at the metal-support interface with Ce cation, gives rise to the strong enhancement of the band at ~ 1965 cm^1, as most of the water desorbs from ceria; in good agreement with Kappers et al. [53]. This "bridged-like" interface species correlates with the enhanced intensity in the C1s region identified as bridged CO. Its pronounced appearance is accompanied by the increase of C-H vibration in DRIFT spectra and accordingly in the XPS C1s region. We suggest that this band at 1960-1970 cm^{-1} is a possible precursor for CO dissociation on the boundary site, and therefore the precursor for methylidyne or hydrogenated graphitic species. At the same time, formate species became more pronounced. If CO does not dissociate at the interface, but rather hops to the ceria, surface formates can be formed in the reaction with OH groups. However in the absence of surface water they accumulate near the Pt particles and represent a "dead-end" for the reaction. The formation of all the above-mentioned (C-H) species shows apparently a negative correlation with the CO_2 production (Figure 12), thus the catalyst is deactivating.

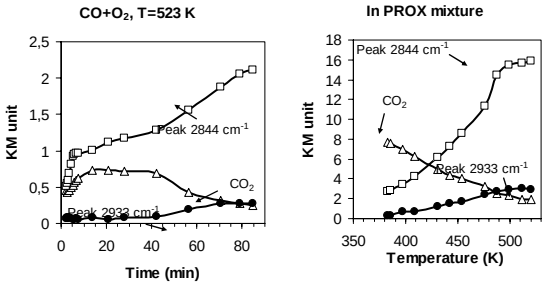

Figure 12: Correlation of integrated intensities of surface C-H bands and gas-phase CO_2 band. Both of them originate from in-situ DRIFTS data and are expressed in Kubelka-Munk (KM) units.

To sum up, the most feasible mechanism for CO oxidation in PROX mixture is as follows. At the beginning, a significant amount of water accumulates on the ceria, via spillover of adsorbed hydrogen atoms from the platinum. This water reacts in LTWGS reaction with *linearly* bonded CO at the Pt/ceria interface, forming CO_2 and hydrogen. This latter, instead of desorption, regenerates surface water by reacting with oxygen. At high T, the hydrogen-bonded structure decomposes and water desorbs. As a result, CO can bind in *bridged-like* manner at the interface, giving rise to dissociation and/or formate formation. Thereafter the empty interface site can be quickly refilled by a new CO molecule continuing this side-reaction. Although surface formates as intermediates in PROX cannot be completely excluded, they seem to play rather the dead-end for the reaction. The key feature appears to be the *linearly* bonded CO at the Pt/ceria interface in a close interaction with surface water.

5. Conclusions, Summary

The preferential oxidation of CO in the presence of excess hydrogen (PROX) on Pt/CeO_2 catalysts was examined by different spectroscopic techniques - DRIFTS and XPS - in combination with catalytic measurements in de-

sired in-situ apparatuses. Characterization of the sample by temperature-programmed-desorption (TDS) and transmission electron microscopy (TEM) gave corresponding results. The first major conclusion of the paper is that the results of these techniques, especially in-situ DRIFTS (surface species) and high-pressure XPS (oxidation states under reaction conditions) perfectly complement each other. The catalytic data of the PROX reaction measured in the two in-situ spectroscopic systems showed identical trends to those determined in the atmospheric catalytic reactor.

The surface species determined by DRIFTS in the presence of CO alone and $CO+O_2$ mixture were very similar to each other. Thus CO oxidation would take place in a similar way in the presence and absence of oxygen, supporting the mechanism of CO oxidation proposed earlier for ceria supported noble metal catalysts. The role of gas phase oxygen is limited to the regeneration of reduced ceria sites. In the presence of hydrogen, however, the carbonate and formate species found by DRIFT spectroscopy during PROX reaction indicate strongly that this reaction differs from CO oxidation.

No resolved OH bands could be found by DRIFT in the PROX reaction mixture indicating a significant amount of adsorbed water on the ceria surface in a hydrogen bonded structure. Its presence seems to suppress hydrogen oxidation while CO oxidation still takes place, as the metallic particles are covered by CO (DRIFTS). On the other hand, no direct correlation between CO coverage and CO_2 formation can be found. The direct contribution of surface water in a low-temperature water-gas-shift (LTWGS) reaction was established, causing apparently high selectivity towards CO oxidation. Increasing temperature leads to a slight decrease in the CO coverage on metal particles, desorption of surface water and increase of formate species. This latter two facts decrease the selectivity towards CO oxidation as a function of temperature.

Earlier attempts about the PROX reaction aimed at suppressing hydrogen adsorption on the catalyst (usually metal) surface, while CO adsorption and oxygen activation (usually on different sites) are possible. Our results point, however, to the beneficial effect of surface water, (i) because it suppresses further hydrogen oxidation and (ii) it can directly participate in the water-gas-shift reaction. Conclusively, one other possible way to prepare a highly selective PROX catalyst is to suppress water desorption (and not water formation) and promote LTWGS reaction. Further investigations are on the way about more realistic (water and CO_2 containing) reaction mixtures.

Acknowledgements

Financial supports by the Hungarian National Science Foundation (Grant OTKA F046216) and from the Athena Consortium are gratefully acknowledged. A. Wootsch thanks the Bolyai Grant of the Hungarian Academy of Sciences for additional financial support. Technical assistance of the BESSY staff during the in-situ XPS measurements is also acknowledged.

References

[1] J. Appleby, F. R. Foulkes, Fuel Cell Handbook, Van Nostrand Reinhold, New York, 1989.
[2] J. N. Armor, Appl. Catal. 176 (1999) 159.
[3] F. Aupretre, C. Descorme, D. Duprez, Catalysis Comm. 3 (2002) 263.
[4] C. D. Dudfield, R. Chen, P. L. Adock, Int. J. Hydrogen Energy 26 (2001) 763.
[5] S. H. Lee, J. Han, K-Y Lee, J. Power Sources 109 (2002) 394.
[6] G. Avgouropoulos, T. Ioannides, Ch. Papadopoulou, J. Batita, S. Hocevar, H. K. Martalis, Catal. Today 75 (2002) 157.
[7] G. K. Bethke, H. H. Kung, Appl. Catal. 194-195 (2000) 43.
[8] M. J. Kahlich, H. Gasteiger, R. J. Behm, J. Catal. 182 (1999) 430.
[9] M. M. Schubert, M. J. Kahlich, H. A. Gasteiger, R. J. Behm, J. Power Sources. 84 (1999) 175.
[10] S. H. Oh, R. M. Sinkevitch, J. Catal. 142 (1993) 254.
[11] M. J. Kahlich, H. A. Gasteiger, R. J. Behm, J. Catal. 171 (1997) 93.
[12] S. Özkara, A. E. Aksoylu, Appl. Catal. A 251 (2003) 75.
[13] A. Wootsch, C. Descorme, D. Duprez, J. Catal. 225 (2004) 259.
[14] Y.-F. Han, M. J. Kahlich, M. Kinne, R. J. Behm, Phys. Chem. Chem. Phys. 4 (2002) 389.
[15] M. M. Schubert, M. J. Kahlich, G. Feldmeyer, M. Hüttner, S. Hackensberg, H. A. Gasteiger, R. J. Behm, Phys. Chem. Chem. Phys. 3 (2001) 1123.
[16] M. Haruta, Catal. Today 36 (1997) 153.
[17] X. Liu, O. Korotkikh, R. Farrauto, Appl. Catal. A 226 (2002) 293.
[18] A. Trovarelli, Catal. Rev. Sci. Eng. 38 (1996) 439.
[19] Y. Y. Yung-Fang, J. Catal. 87 (1984) 162.
[20] S. Johansson, L. Österlund, B. Kasemo, J. Catal. 201 (2001) 275.
[21] R. Taha, D. Martin, S. Kacimi, D. Duprez, Catal. Today 29 (1996) 89.
[22] T. Bunluesin, H. Cordatos, R. J. Gorte, J. Catal. 157 (1995) 222.
[23] E. Bekyarova, P. Fornasiero, J. Kaspar, M. Graziani, Catalysis Today 45 (1998) 179 .
[24] H. C. Yao, Y. F. Yu-Yao, J. Catal. 86 (1984) 254.
[25] S. Bedrane, C. Descorme, D. Duprez, Catalysis Today 73 (2002) 233.

[26] S. Bedrane, C. Descorme, D. Duprez, Catalysis Today 75 (2002) 401.
[27] S. Bernal, J. J. Calvino, G. A. Cifredo, J. M. Rodriguez-Izquierdo, V. Perrichon, A. Laachir, J. Catal. 137 (1992) 1.
[28] S. Salasc, V. Perrichon, M. Primet, M. Chevrier, N. Mouaddib-Moral, J. Catal. 189 (2000) 401.
[29] S. Bernal, J. J. Calvino, M. A. Cauqui, J. M. Gatica, C. Larese, J. A. Pérez Omil, J. M. Pintado, Catal. Today 50 (1999) 175.
[30] W. J. Shen, Y. Ichihashi, H. Ando, Y. Matsumara, M. Okumura, M. Haruta, Appl. Catal. A 217 (2001) 231.
[31] G. Rupprechter, J. J. Calvino, C. López-Cartez, M. Fuchs, J. M. Gatica, J. A. Pérez-Omil, K. Hayek, S. Bernal, Stud. Surf. Sci. Catal. 130 (2000) 2021.
[32] A. Holmgren, B. Andersson, D. Duprez, Appl. Catal. B 22 (1999) 215.
[33] C. Binet, M. Daturi, J.-C. Lavalley, Catal. Today 50 (1999) 207.
[34] D. W. Daniel, J. Phys. Chem 92 (1988) 3891.
[35] T. Jin, Y. Zhou, G. J. Mains, J. M. White, J. Phys. Chem 91 (1987) 5931.
[36] C. Li, T. Arai, K. Domen, K. Maruya, T. Onishi, J. Chem. Soc., Faraday Trans. 85 (1989) 929.
[37] C. Li, Y. Sakata, T. Arai, K. Domen, K. Maruya, T. Onishi, J. Chem. Soc., Faraday Trans. 85 (1989) 1451.
[38] A. Pfau, K. D. Schierbaum, Surf. Sci. 321 (1994) 71.
[39] A. Q. Wang, P. Punchaipetch, R. M. Wallace, T. D. Golden, J. Vac. Sci. Technol. B 21 (2003) 1169.
[40] M. A. Henderson, C. L. Perkins, M. H. Engelhard, S. Thevuthasan, C. H. F. Peden, Surf. Sci. 526 (2003) 1.
[41] Y. Madier, C. Descorme, A. M. Le Govic, D. Duprez, J. Phys. Chem. B. 103 (1999) 10999.
[42] D. Teschner, A. Wootsch, K. Matusek, T. Röder, Z. Paál, Solid State Ionics 141 (2001) 709.
[43] S. Kacimi, J. Barbier Jr., R. Taha, D. Duprez, Catal. Lett. 22 (1993) 343.
[44] A. Holmgren, B. Andersson, J. Catal. 178 (1998) 14.
[45] D. F. Ogletree, H. Bluhm, G. Lebedev, C. Fadley, Z. Hussain, M. Salmeron, Rev. Sci. Instrum. 73 (2002) 3872.
[46] D. Teschner, A. Pestryakov, E. Kleimenov, M. Hävecker, H. Bluhm, H. Sauer, A. Knop-Gericke, R. Schlögl, J. Catal. 230 (2005) 186.
[47] D. Teschner, A. Pestryakov, E. Kleimenov, M. Hävecker, H. Bluhm, H. Sauer, A. Knop-Gericke, R. Schlögl, J. Catal. 230 (2005) 195.
[48] [P. Burroughs, A. Hamnett, A. F. Orchard, G. Thornton, J. Chem. Soc. Dalton Trans. 17 (1976) 1686.
[49] D. Ferri, T. Bürgi, A. Baiker, Phys. Chem. Chem. Phys. 4 (2002) 2667.
[50] R. Barth, R. Pitchai, R. L. Anderson, X. E. Verykios, J. Catal. 115 (1989) 61.
[51] J. Silvestre-Albero, A. Sepulveda-Escribano, F. Rodriguez-Reinoso, J. A. Anderson, Phys. Chem. Chem. Phys. 5 (2003) 208.
[52] P. Hollins, Surf. Sci. Rep. 16 (1992) 51.
[53] M. J. Kappers, J. T. Miller, D. C. Koningsberger, J. Phys. Chem. 100 (1996) 3227.
[54] F. Bonzon-Verduraz, A. Bensalem, J. Chem. Soc. Faraday Trans. I 90 (1994) 653.
[55] T. Shido, Y. Iwasawa, J. Catal. 136 (1992) 493.
[56] C. Binet, M. Daturi, J. C. Lavalley, Catal. Today 50 (1999) 207.
[57] A. Tsyganenko, V. Filimonov, J. Mol. Struct. 19 (1973) 579.
[58] A. Badri, C. Binet, J. C. Lavalley, J. Chem. Soc., Faraday Trans. 92 (1996) 4669.
[59] A. Laachir, V. Perrichon, A. Badri, J. Lamotte, E. Chaterine, J. C. Lavalley, J. El Fallah, L. Hilaire, F. Le Normand, E. Quemere, G. N. Sauvion, O. Touret, J. Chem. Soc., Faraday Trans. 87 (1991) 1601.
[60] K. Nakamoto. "IR and Raman Spectra of Inorganic and Coordination Compounds, Wiley-Interscience, New York, 1987.
[61] G. Busca, J. Lamotte, J. C. Lavalley, V. Lorinzelli, J. Am. Chem. Soc. 109 (1987) 5197.
[62] C. Li, K. Domen, K. Maruya, T. Onishi, J. Catal. 125 (1990) 445.
[63] G. Jacobs, U. M. Graham, E. Chenu, P. M. Patterson, A. Dozier, B. H. Davis, J. Catal. 229 (2005) 499.
[64] M.-C. Jung, H.-D. Kim, M. Han, W. Jo, D.C. Kim, Jpn. J. Appl. Phys. 38 (1999) 4872.
[65] J. S. Hammond, N. Winograd, J. Electrochem. Electroanal. Chem. 78 (1977) 55.
[66] K. S. Kim, N. Winograd, R. E. Davis, J. Am. Chem. Soc. 93 (1971) 6296.
[67] C. R. Parkinson, M. Walker, C. F. McConville, Surf. Sci. 545 (2003) 19.
[68] J. L. G. Fierro, J. M. Palacios, F. Tomas, Surf. Interface Anal. 13 (1988) 25.
[69] K. Dückers, K. C. Price, H. P. Bonzel, V. Chab, K. Horn, Phys. Rev. B 36 (1987) 6292.
[70] N. M. Rodriguez, P. E. Anderson, A. Wootsch, U. Wild, R. Schlögl, Z. Paál, J. Catal., 197 (2001) 365
[71] S. Bernal, J. J. Calvino, G. A. Cifredo, J. M. Gatica, J. A. P. Omil, J. M. Pintado, J. Chem. Soc. Faraday Trans. 89 (1993) 3499.
[72] A. B. Mhadeswar and D. G. Vlachos, J. Phys Chem. B. 108 (2004) 15246.
[73] G. Jacobs, P. A. Patterson, U. M. Graham, D. E. Sparks, B. H. Davis, Appl. Catal. A 269 (2004) 63.